Sādhanā (2021)46:53
https://doi.org/10.1007/s12046-021-01571-x

Experiments on unsteady pool fires – effects of fuel depth, pan size and wall material

A SHIVA KUMAR*, A V E SOWRIRAAJAN, C S BHASKAR DIXIT and H S MUKUNDA

Fire and Combustion Research Center, Jain Deemed to be University, Kanakapura Road, Bangalore, India
e-mail: shivakumarannaiappa@gmail.com; sowrirajan.venugopalan@gmail.com; bhaskar.dixit@gmail.com; hsm.cgpl@gmail.com

MS received 7 January 2020; revised 23 October 2020; accepted 17 December 2020

Abstract. This paper presents specifically designed experiments to understand the effect of range of parameters on pool burn behavior with liquid fuels. Experiments have been conducted on pool fires with 0.1–2 m diameter pans and depths of 40, 50, 60 and 90 mm with n-heptane fuel depths up to 30 mm floated on water and without water in an indoor fire laboratory. Pans of 0.2 m dia are made of glass, stainless steel, mild steel and aluminum and larger diameter pans only of mild steel. The experiments conducted include some with fuel initial temperature effects at 300, 319 and 343 K. Data on temporal evolution of mass burn, pan wall temperatures, temperatures inside the liquid at some depths and gas phase temperatures at select heights from the pool surface have been obtained from the experiments. Results show that at larger fuel depths of ($\sim$ 30 mm), a burn mass flux of 60–75 g/m^{2}s is reached even in 0.2 m dia pans. This flux is expected only in large pans of about 2 m size. Regarding pan material effect, glass pans show mildly increasing low flux values (10–15 g/m^{2}s) and mild steel and aluminum pans show an initial low flux value ($\sim$ 10 g/m^{2}s) and then a sharp change to large flux values depending on the depth. At larger depths, the flux values go up to 65 g/m^{2}s. In case of stainless steel, the mass flux variation occurs smoothly all through towards increasing values. As regards the water depth below the fuel, the decrease in the average burn rate is about 1 % per mm water depth up to 20 mm for all pans with diameter below 0.5 m. Larger size pans with burn rate controlled largely by radiation show much reduced effect of the water depth. In order to correlate the data with diverse parameters a dimensionless number, *Mpc*, has been invoked using scaling laws, and a correlation that provides a good estimate of the mass burn flux including all the effects considered earlier has been deduced. The data set thus generated provides the basis for a more detailed model to predict the mass loss history and other parameters.

Keywords. Pan fire; burn rate; scaling laws.

1. Introduction

Pool fire has been a subject of study for six decades from the time Hottel [1] published a review of the Russian work. Considerable information and understanding has been gained over this period with research, fire safety technology and evolution of standards for acceptance of fire safety products having made great progress. One of the key questions of importance is the prediction of burn rates from liquid pool fires, particularly because pool fires are a part of the standards for fire extinguishment and hence fire safety product qualification, since several of these tests use the burn of a fixed depth of fuel over water (like Underwriter laboratories standard UL162, for instance, uses 2″ of fuel over 2″ of water with 8″ of free board). Although unsteady burn process is the basis of these tests, most investigators have used steady arrangement to study the burn rate of liquid pool fires both experimentally and for model development. Hottel [1] has reviewed pan fire experimental data published by Blinov and Khudiakov [2] in Russian language. This review is widely referred to by fire community. Babrauskas [3] summarized the burn rate data from several sources for a number of fuels. He brought out that transient effects due to lip height (or free board), the nature of bounding material, fuel layer thickness and wind would need to be accounted.

The effects of wall material are known to be dominant in relatively small pool fires (generally below 200 mm pan diameter). Small pool fires have been studied by Hayasaka [4] and Chen *et al* [5, 6], particularly in the unsteady mode – with fixed fuel thickness. Interesting experiments were carried out by Hayasaka [4] on small pool fires of 50 mm dia and 11 mm n-heptane with measurements of mass loss and wall temperature as well as liquid temperature. Chen

*For correspondence
Published online: 10 March 2021

et al [5] and Chen *et al* [6] performed experiments at ambient temperature and different fuel temperatures both on 200 mm dia pan of 40 mm depth with 6 and 13 mm n-heptane. These insightful experiments, in which measurements of liquid temperature at various depths as well as outer wall temperatures at select distances from the top are made, show different regimes of combustion – in fact four different phases, with the maximum fuel flux when the remaining liquid fuel layer reaches boiling. Admittedly, every unsteady liquid pool fire will undergo most of these changes and they need to be factored into any model intending to describe the fuel burn behavior. Also a single burn rate defined as the fuel thickness divided by the time of burn may be a useful overall indicator of the burn rate, but would be inadequate to capture the burn behavior since the burn rate increases as one proceeds from ignition to end of burn. The only way of capturing such a behavior would be to treat the process as unsteady, and track the burn process as the governing parameters change. Nakakuki [7, 8] has performed complex calculations towards obtaining the heat balance in a pool fire with different pan materials and fuels, with a large number of assumptions. One of the interesting experimental results he has reported is that self-quenching occurs at free board values comparable in magnitude to the diameter of the pan (d_{pan}). Thus, free board effects for larger diameter pools (more than 100 mm) with free board values less than 30 $\%d_{pan}$ can be considered to be negligible. Dlugogorski and Wilson [9] have studied lip effects on burn rate in very small pool fires, and have shown extinction beyond a certain lip height-to-diameter ratio.

Hamins *et al* [10] use a steady configuration of ring burners to obtain various pool diameters (77–300 mm) and they use several fuels, including n-heptane and toluene, to measure the burn rates and radiational characteristics as a function of radius and azimuth, and their principal conclusion is that the flux is fairly uniform for hydrocarbon fires. Klassen and Gore [11] provide details of the results [10] in their NIST report.

There are a much larger number of experiments on large pool fires [12–16] with measurements of burn rate as well as thermal features. Gregory *et al* [12] reported burn rate and fire temperature measurements on a hydrocarbon-over-water fire in a pan of 9.1 m x 18.3 m x 0.9 m deep concrete pool with fuel depths of 220 and 190 mm over 660 mm water burning for 35 and 29 min. The measured fuel fluxes are about 80–85 g/m^{2}s and gas temperatures about 1300 $\pm$ 50 K at 1.42 m above the pool (16 % of the width) with a fair amount of intermittency. At 0.26 m height, the temperature drops to 1000 $\pm$ 150 K with variations about mean at very low frequency. Koseki [13] summarizes the experimental results of the fire research institute of Japan concentrating on pool fires on large pans. Heptane and other fuels have been studied on large diameter pools with fuel floating over with free board of 30–50 mm. Mean burn rates as a function of pool diameter show that heptane has the largest burn flux followed by gasoline and kerosene. Measured flame temperatures for n-heptane show an increase of peak temperature (on the axis) from 1150 K for 0.3 m pan to 1300 K for 3 m pan, a feature that appears puzzling. Other fuels show larger temperatures (1650 K) at larger diameters. Hayasaka [14] made measurements of radiational flux on a 2.7 m x 2.7 m pool fire with 20–30 mm thick n-heptane and other fuels. With burn fluxes of 81, 39.5 and 38.3 g/m^{2}s, their measurements have shown that the radiant flux from a zone termed "quasi-flame and vortex" region that is near the high-temperature zone is higher for n-heptane than for kerosene and crude oil. Blanchet and Anttilla [15] have performed useful and interesting experiments with n-heptane, toluene, methanol, ethanol and some mixtures on a variety of issues surrounding the features of pool burn behavior. Radiation absorptions through the fuel vapor as well as beneath the liquid surface have been measured and the results show dependence on the fuel. Experiments without and with glass (GL) beads in the liquid zone show that the convection inside the fuel has marginal influence on the burn rate flux. Radiation absorption by the top layer of fuel is limited to about 3 mm.

Ditch *et al* [16] have pursued producing an empirical correlation over a large number of fuels – many of them synthetic, to create a range of fuels with different properties controlling the burn rate. The key parameters in the model are the latent heat of vaporization and smoke point of the fuel. The correlation is shown to work well for many fuels. It is unclear why the correlation does not benefit from appropriate dimensionless parameters, even if it is empirical.

A careful examination of these studies shows that a broad understanding of the physics is available. All pool fires are controlled by three mechanisms of heat transfer – conduction via walls of the pan, which depends on the material of the pan and its geometry, convective and radiative heat transfer from the flame over the fuel surface. The relative effect of convective and radiative heat transfer vis-a-vis conduction heat transfer is controlled by fuel surface area to pan diameter times pan height/wall thickness. For systems used in practice, it can be taken as the ratio of pan-diameter-to-pan height/wall thickness. Thus as pan diameter increases, the role of conduction heat transfer decreases. Also radiation heat transfer increases with the pan diameter, which controls the size of the fire, and convective heat transfer has a weak dependence on pan diameter (it will be shown very specifically in this paper that the convective heat transfer coefficient is a constant value over wide parameter range). Thus the broad conclusion from the literature is that large pool fires are controlled by radiation and small fires by geometrical features and the pan material. Unfortunately, the literature is abound with data and the reported mass flux values for similar pan fires by

different authors differ considerably. A quantitative assessment of reasons for the difference is not available. Babruskas [3] has expressed a need for rationalization as early as in 1983. It is therefore the aim of this study to elucidate the various effects more particularly on n-heptane as it is considered to be a standard fuel in many fire standards for the qualification of foams.

2. Present study

In view of the earlier discussion, the present study has two aims:

1. Conduct of a sequence of experiments to elucidate the effects of free board (h_{fb}), wall material properties – density (ρ_w), specific heat (c_{pw}), conductivity (k_w), thickness (t_w), depth (h_{pan}), fuels with their physical and thermal properties – density (ρ_{fu}), specific heat (c_{pfu}), boiling point (T_{bfu}), latent heat of phase transformation (L_{fu}), conductivity (k_{fu}) and depth (h_{fu}) at different initial temperatures (T_0), stoichiometric ratio with air (S), fire temperature with the oxidant, namely air (T_f), and circular pans with diameters of 0.1–2.0 m.
2. Evolving of a dimensionless number (M_{pc}) that involves the geometric, thermodynamic and transport properties that can characterize the mean burn behavior defined by the burn mass flux ($\bar{m}''_{fu}$).

The present paper focuses attention only on n-heptane as the fuel even though experimental data have been obtained on other fuels because (a) it is a "standard" fuel used in foam qualification tests and (b) its burn mass flux is very large in comparison with several other fuels like kerosene and diesel where the conduction effects are not as dominant. It is recognized that the number of parameters controlling the burn mass flux is large and in order to delineate their effects, a large number of carefully designed experiments are performed. In this study, 60 experiments were conducted at ambient temperature with fuel thicknesses of 10, 13, 20 and 30 mm in pan diameters of 0.2–2 m. Effects of fuel thickness, free board, pan material and pan diameter on the burn rate of fuel are quantified. Several more experiments on fuel floated on water in 0.2 and 0.5 m pans are conducted to uncover the effect of water on mass flux. A few experiments on initial fuel temperature effects were also conducted.

3. Experimental arrangement

The experimental arrangement consisted of small and large pans in order to extract free board effect and wall conduction effect. Pans of 40, 50, 60 mm depth with 0.2, 0.3, 0.4 and 0.5 m dia made of 3 mm thick mild steel (MS) were fabricated. The pans with different depths could be used to evaluate the effects of free board. Pans of 0.1 and 0.2 m dia, 40 mm depth and 3 mm thick stainless steel (SS) were also fabricated and used in experiments to replicate the results of Chen *et al* [5, 6]. Figure 1 shows several of the pans used in this study.

Figure 2 shows diagrammatically the arrangements for the measurement of mass, wall temperatures and temperatures within the liquid at the centerline and gas temperatures. K-type thermocouples of 0.4 mm bead size are used. The mounting of the thermocouple wires was through ceramic tubes with an exposed region of 5 mm. The pan itself is placed over an Alumini-silicate blanket of 25 mm thickness that rests over a balance of 5 kg capacity with an accuracy of 100 mg for small pan fire tests and a balance of 60 and 1000 kg capacity with an accuracy, respectively, of 1 and 10 g for larger pans. For extracting initial fuel temperature effects, the pan and fuel were heated and brought to the desired temperature before the start of the experiment. T_p and T_{wb} are, respectively, the pan tip and the bottom outer region temperatures measured; h_{fu} and h_{fb} in figure 2 indicate the fuel depth used and the free board height. These experiments were restricted to fuel temperatures above the local ambient to avoid ambient moisture condensation on colder pan surfaces. The experiments were conducted near the center of a large 18 m x 12 m x 12 m indoor fire facility with a special construction to ensure minimal ambient disturbances. Measured ambient disturbances were less than 0.2 m/s and flames always showed symmetry expected of quiescent environment. Figure 3 shows the flame structure for 0.2 and 2 m pan pool fire experiments. In the 0.2 m pan the role of pan wall conduction heat feed back to fuel will be high compared with other two modes of heat transfer whereas in the case of 2 m pan the radiation is the dominant heat transfer mode.

4. Results

The first set of experiments was devoted to a comparison to the work of Chen *et al* [5, 6]. The plot of fuel mass vs time of present experiments with SS pan along with those of Chen *et al* [5, 6] appears in figure 4. The experimental data of Chen *et al* [5] are at much lower fuel temperatures, perhaps related to the local ambient temperature. Our attempt to replicate the experiments at the same temperature was made difficult because of the condensation of moisture and hence, the experiments were limited to the ambient temperature. The initial mass loss matches well and the later mass loss is different due to ambient temperature effects. At h_{fu} = 20 mm, it can be seen that the peak fuel flux ($\dot{m}''_{fu}$) reaches large values up to 37 g/m^{2}s.

To further investigate the issue, experiments were carried out on 0.2 m dia MS pan with 3 mm wall thickness. The results are set out in figure 5. It can be seen that mass loss

Figure 1. Pans of 200 mm dia, 40 mm depth made of stainless steel (SS), mild steel (MS), aluminum alloy (AL) and glass (GL) (clockwise from the top) on left side and pans of 300, 400 and 500 mm dia, 40, 50 and 60 mm depth made of MS on the right side.

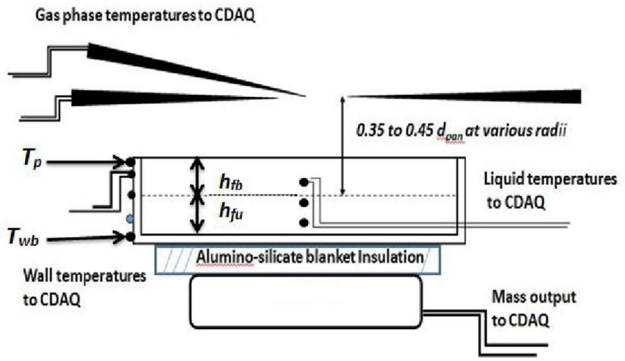

Figure 2. Experimental arrangement used in the experiments to include mass loss, wall, gas and liquid temperatures during the burn.

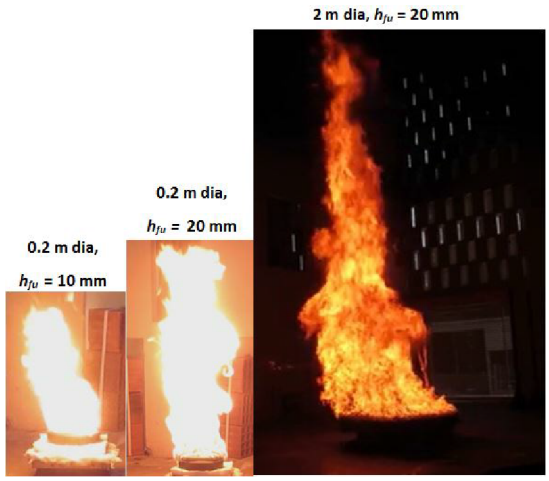

Figure 3. Flame structure of pool fire experiment performed in 0.2 m MS pan at a fuel depth 10 and 20 mm and 2 m MS pan at a fuel depth of 20 mm.

curve has two segments – initial one that seems similar in slope that gives $\dot{m}''_{fu}$ (after dividing by the pan area) and a later one in which the burn rate is significantly larger. At 5 mm fuel depth, $\dot{m}''_{fu}$ of 24.5 g/m^{2}s is similar to the value obtained by Chen *et al* [5, 6]; however, at higher depths, $\dot{m}''_{fu}$ values go up to 60 and 67.3 g/m^{2}s at 20 and 30 mm depth. It appears that the burn behavior has reached a steady value at this stage. These values are similar to the mass flux values achieved in large pool fires. A quick inference is that this behavior is related to the liquid in the pool having reached boiling, a feature that needs further investigation.

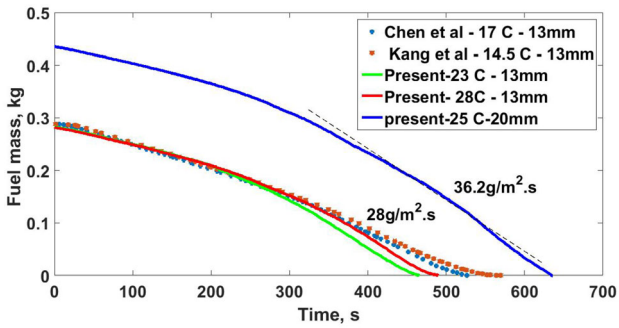

Figure 4. Comparison of mass loss with time for 0.2 m SS pans, 40 mm deep with Chen *et al* [5] for 13 mm n-heptane; also 20 mm heptane, present.

At this stage, it is thought useful to examine the burn behavior with pans of different materials. Figure 6 presents mass loss with time for pans of different materials. The mass loss rate for GL pan varies slightly over the burn time; for SS pan it increases smoothly over the burn duration; for MS and AL pans, it changes very significantly with a sharp change at a time that for AL pan is ahead of MS. If we note that thermal conductivity of these materials is in an increasing order (see later for data), it can be inferred that wall heat transfer process must be affecting the behavior directly. In order to clarify this feature experimentally,

another MS pan was fabricated with a 20 mm channel all around the pan side (of 60 mm depth). Two experiments of n-heptane burn with this pan without and with ambient water circulation were performed. The results are set out in figure 7. As can be noted, for the case without water flow, one has the two-segment $\dot{m}''_{fu}$ behavior and with water flow, it is about 12 g/m^{2}s except for the initial transient. The initial transient is due to water temperature being slightly higher than the temperature of the fuel.

In order to understand the thermal behavior, each of the pans had thermocouples mounted at the bottom outer region (T_{wb}) and near the tip of the pan (T_p). In select experiments, thermocouples were placed at other locations in-between as well. In each of the cases, a 400 micron K type thermocouple was welded after creating a small dent at the marked location. The results of T_{wb} for all the cases on 0.2 m dia pans of different materials are set out in figure 8. The left side figure is set with time coordinate. While the general tendency of faster rise with AL and MS pans is clear when observed carefully, the right side plot of T_{wb} with a fuel regression (reg) rendered dimensionless by the initial fuel thickness, h_{fu}, as $z = reg/h_{fu}$ for these experiments makes the differences in the behavior more clear. The group of plots on the lower end belongs to GL and SS pans – the arrival of heat via the pan wall occurs slowly with these pans. The group with sharper initial rise belongs to MS and AL. Another deduction is that a substantial regression for these pans occurs at higher temperatures, implying that the pool has reached near boiling conditions earlier in these cases.

In order to explicitly extract this feature, the temperature at the center of the pan, 1 mm above the bottom inside the fuel denoted T_{bo} is set out for pans of all materials for a fuel depth of 20 mm in figure 9. The rise in the liquid temperature is the fastest with pans of higher thermal conductivity. The true origin for this behavior lies in the fact that the gas phase heat flux is much higher in these cases and hence, the heat flux transferred to the liquid is much higher. This controls the heat flux into the liquid. In each of the cases the liquid reaches a temperature near the boiling point and

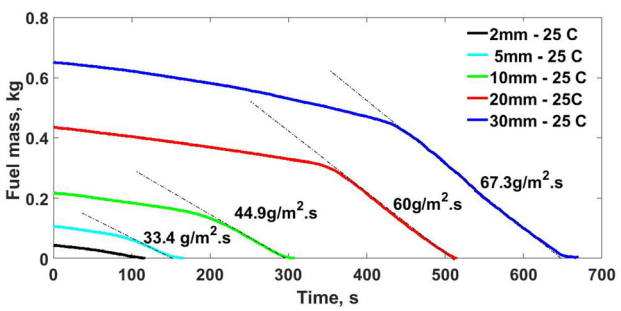

Figure 5. Mass loss with time on a 0.2 m dia MS pan, 40 mm deep with 5–30 mm n-heptane.

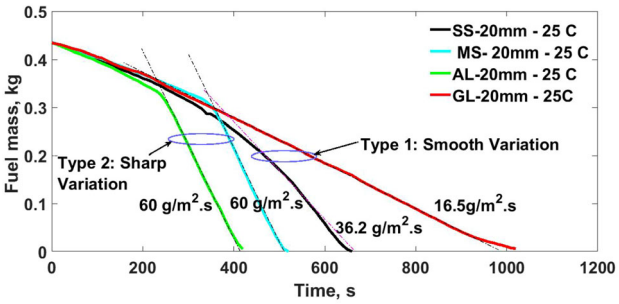

Figure 6. Mass loss with time on 0.2 m dia pans of different materials, 40 mm deep with 20 mm n-heptane.

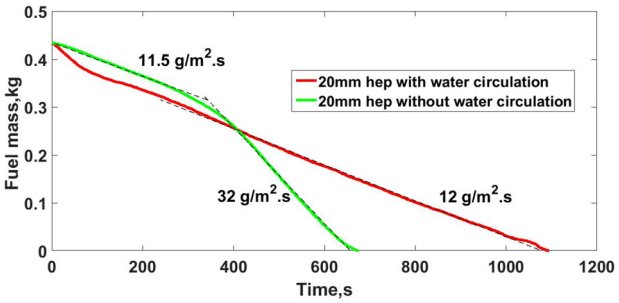

Figure 7. Mass loss with time on a 200 mm dia MS pan with and without water circulation around the side with the uncooled pan bottom resting on ceramic blanket; 20 mm hep implies 20 mm n-heptane fuel depth.

levels off, indicating that the burn process during this period occurs with the liquid in bulk boiling mode.

Figure 10 shows the variation of the pan tip temperature, T_p, and the bottom outer wall temperature, T_{wb}, for pans of different materials. Pan tip temperature is chosen as an important candidate for describing the burn behavior as the pan tip receives the heat from the flame just above it and transfers it along the pan to the bottom region. Pans with lower thermal conductivity reach higher tip temperatures and lower bottom wall temperatures (see the variation for

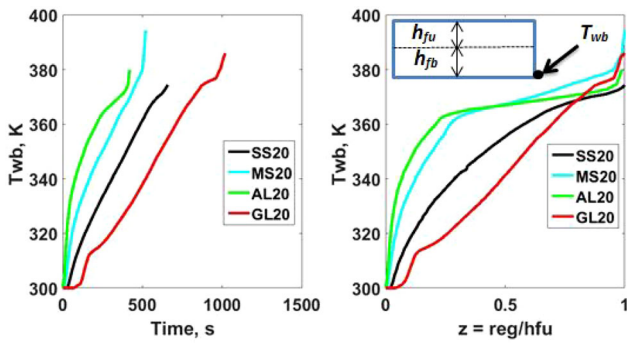

Figure 8. Bottom outer wall temperature, T_{wb}, on 200 mm dia 40 mm deep pans of AL, MS, SS and GL materials for 20 mm fuel depth.

GL pan, in particular). The pan tip temperatures seem to level off for a reasonable time before they begin to increase later. The actual values of T_p during the "steady" regime are about 370 K for AL – just above the boiling point of n-heptane, 390–400 K for MS, 430–440 K for SS and 530–540 K for GL. These features are important and will aid the development of the mathematical model for predicting the burn behavior.

The measured wall temperatures at specific points on the wall (T_{wall}) are set out in figure 11 for MS and SS pans. It appears that to a first order, the behavior of T_{wall} with distance along the wall can be considered linear. This trend is similar to the one observed by Chen *et al* [6].

Experiments on 0.5 m dia MS pan have been conducted with different fuel thicknesses, as also with pans of different depths to extract the free board influence. The results are set out in figure 12. As can be noted the burn rates are higher (because the burn times are much lower than for 0.2 m dia pan) and the influence of free board seems small – less than 5 % within the accuracy of the experiments.

In order to understand the effect of water depth on the burn rate of fuel that floats over water, experiments were conducted with 0.2 and 0.5 m dia MS pans. The choices of fuel and water depths were made such that free board was kept constant and hence, the effect of water could be extracted separately. Figure 13 shows the mass loss variation of experiments with only fuel and fuel floated on water. It can be observed that, at the initial stage, burn rate remains same and the deviations occur later. Figure 14 shows variation of burn rate of 0.5 m MS pan with 10 mm fuel floated on the different thicknesses of water; it is evident that even though the initial burn rate does not vary for significant amount of time the maximum and mean burn rate decrease with increasing thickness of water. In this particular plot, the free board changes because the total depths of fuel and water increase. A calculation of the changes in the mean burn flux shows that up to 0.5 m dia pan, the decrease can be estimated at 1 % per mm water thickness up to 20 mm water thickness. For larger diameter

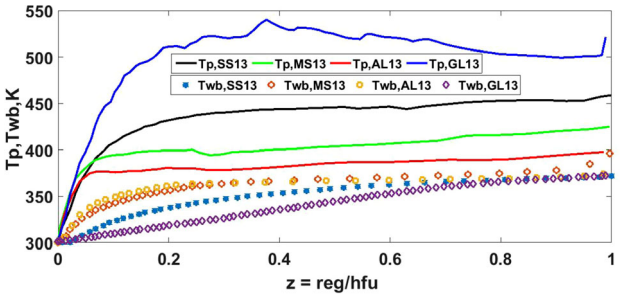

Figure 10. The pan tip temperature, T_p, and the bottom outer wall temperature, T_{wb}, for 0.2 m dia pans of different materials at a fuel depth of 13 mm.

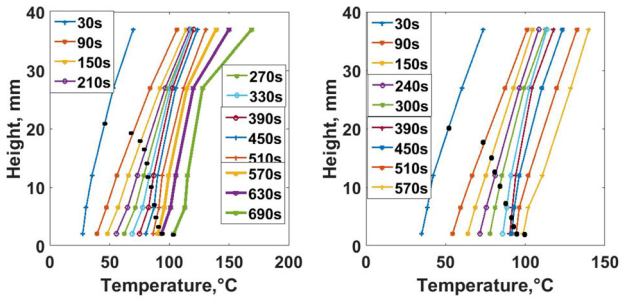

Figure 11. The wall temperature, T_{wall}, for 0.2 m dia pans of SS (left) and MS (right) for h_{fu} = 20 mm as a function of distance from tip to bottom at 60 s time intervals. The dotted lines show the position of liquid surface during the burn.

pans, the difference is within the error band of the fuel burn mass flux ($\sim$ 5 %).

The data from various experiments are summarized in Table 1. The mean flux ($\bar{m}''_{fu}$) ratio shown in this table is obtained as the fuel mass divided by the burn time and pan cross sectional area. Also shown is the peak flux obtained from the increased burn rate after a couple of hundred seconds during which the liquid heats up towards boiling

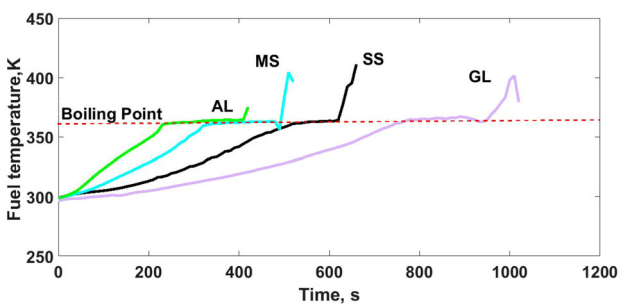

Figure 9. Liquid temperature 1 mm above the pan bottom on the centerline, T_{bo}, on 0.2 m dia 40 mm deep pans of AL, MS, SS and GL materials for n-heptane fuel depth of 20 mm.

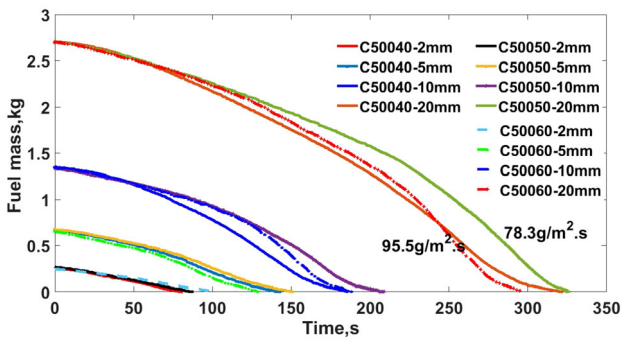

Figure 12. Burn mass loss with time on a 0.5 m dia MS pan, 40, 50, 60 mm deep with 2–20 mm fuel thickness without water; C50040-2 mm implies 0.5 m dia pan, 40 mm pan depth and 2 mm fuel depth.

with heat flux from the gas phase as well as wall conduction. What is clear from the table is that at each pan diameter, both the mean and peak flux increase with the depth with a tendency to reach asymptotic values. Also the material of the pan – MS or SS here – matters significantly in terms of the burn behavior.

A further confirmation to wall conduction effects was seen in the videos taken of these fires showing that after some burn time, the fires become broad with sporadic spewing of the vapors from the side. The flames occasionally turn around and lick the outer regions of the pan, indicating direct heating of the pan. This behavior is not uniform all around and occurs sporadically. Since it is already known that the liquid reaches boiling (shown in figure 9), the wall heat transfer process must be reaching regimes of nucleate boiling (as also pointed out in ref. [6]) with very significant unsteady heat transfer into the fuel. Any approach to modeling the burn process must include these phenomena.

5. Thermal properties of wall material and fuel

Table 2 presents the data on the pan wall materials considered. Several thermal properties of the pan were obtained from data sheets; however thermal conductivity, which is a more sensitive property of the composition, was experimentally obtained by measuring a one-dimensional temperature profile and extracting thermal conductivity from the data. The data matched with information from published sources excepting for AL. In this case it turned out to be an alloy whose precise composition could not be obtained from production sources, and the measured value of k_w = 60 W/m K is very different from published values (120–200 W/m K). Nevertheless, it is much higher than that of MS. If we make a simple estimate of the transient conduction times using $t_{cond} \sim h_{pan}^2/8\alpha_w$, we get the values set out in the last column. Except for GL, the transient conduction times are small compared with the burn time. This implies that steady conduction process along the wall will be a good approximation. Hence, the resulting profile is linear as noted in the wall temperature plots (figure 11).

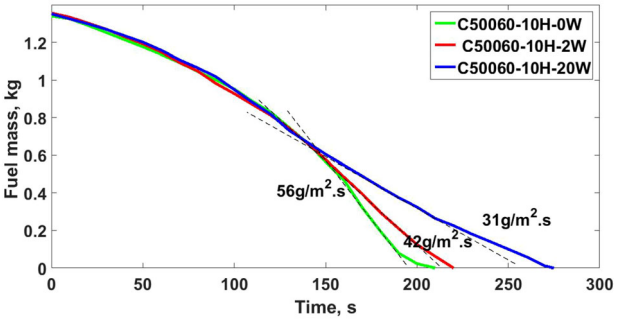

Figure 14. Burn mass loss with time of a 500 mm dia MS pan, 60 mm deep with 10 mm fuel without water and those floated on 2 and 20 mm water; C50060-10H-0W implies 0.5 m dia pan with 60 mm pan depth, 10 mm heptane depth and 0 mm water.

The thermodynamic and transport properties of n-heptane are set out in Table 3. Thermal diffusivity of the liquid is an order of magnitude lower than that of the pan material and hence the heat transfer process through the liquid has to account for unsteady process. The value of T_f set out in Table 3 is that measured in experiments and deserves discussion. As indicated in the earlier section, several investigators (see ref. [13]) have presented various values. It appears from the work of Weckman and Strong [17] that the measured peak temperature and its variation across the pan depend on the fuel. The observation of Koseki [13] that the peak temperature of n-heptane pool fires increased with pan diameter was considered puzzling as already stated. To understand this behavior, K-type thermocouples of 0.4 mm bead diameter with long enough support rod were introduced into the fires from pans of 0.2, 0.5 and 2 m. It was uncovered that introducing a cold thermocouple into the fire resulted in temperature of 850 C (1120 K) and on withdrawal, fair amount of sooting on the thermocouple bead and the leading support was observed. Inferring that the cold wire resulted in immediate soot deposition, the thermocouple was heated to flame temperatures in a separate lean high-temperature LPG flame and then was quickly introduced. This resulted in temperatures of 950 C (1220 K) for about 10 s, after which it started decreasing slowly.

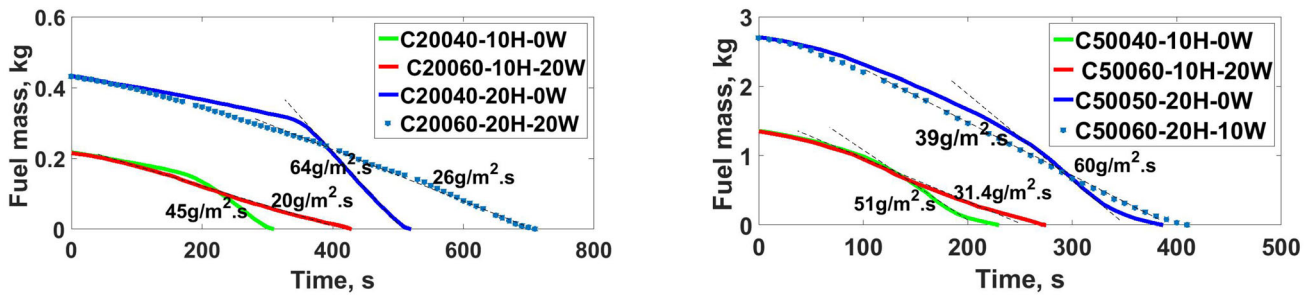

Figure 13. Mass loss vs time of 0.2 and 0.5 m MS pans with fuel without and with water; C50040-10H-20W implies 0.5 m dia pan with 40 mm pan depth, 10 mm heptane depth and 20 mm water.

Table 1. Mean and peak burn rate fluxes (g/m^{2}s) for 0.2, 0.5 and 2 m dia pans; burn rate accurate to ± 5 %.

Flux for h_{fu} (mm) =	2	5	10	20	30
SS pan 0.2 m dia, 40 mm deep					
Mean	11.5	16.2	17.8	25.0	28.9
Peak	14.0	20.1	25.7	34.4	41.0
MS pan 0.2 m dia, 40 mm deep					
Mean	13.1	22.3	26.6	29.8	34.0
Peak	14.6	33.0	42.5	58.1	67.2
MS pan 0.2 m dia, 60 mm deep					
Mean	–	–	–	34	37.3
Peak	–	–	–	58.7	64
MS pan 0.5 m dia, 60 mm deep					
Mean	–	19.9	34.0	40.2	–
Peak	–	22.8	56.4	66.0	–
MS pan 0.5 m dia, 50 mm deep					
Mean	15.3	22.6	32.0	40.9	–
Peak	16.3	29.6	57.8	72.9	–
MS pan 0.5 m dia, 40 mm deep					
Mean	15.9	23.5	37.0	44.6	–
Peak	18.9	32.4	54.2	74.0	–
MS pan 2 m dia, 60 mm deep					
Mean	–	–	–	56.2	–
Peak	–	–	–	73.2	–
MS pan 2 m dia, 90 mm deep					
Mean	–	–	–	58.5	–
Peak	–	–	–	72.4	–

Again withdrawal of the thermocouple showed slight sooting. The inference from these trials was that pre-heated beads would help alleviate the soot-related problems. The data on fire temperature are considered important since they are directly involved in the estimation of convective and radiation fluxes. The influences of chemistry in the fuel rich region above the pan in affecting the sooty composition, the associated peak temperature achieved and the amount of radiation flux reaching the fuel surface are simplified into the use of fire temperature fluctuating around a mean measured value. The measured temperature corrected for radiation is 1200 K and is independent of the pan diameter. The data for n-heptane are summarized in Table 3.

6. Correlation of mean mass flux with M_{pc}

The evolution of a dimensionless number for defining pan conduction M_{pc} to account for the burn rate behavior should involve the following aspects:

- Increase in wall material thermal conductivity (k_w) should increase the heat transfer into the pan and hence increase M_{pc}.
- Increase in free board (h_{fb}) and pan depth (h_{pan}) should reduce the heat transfer and hence M_{pc}. The effect of free board is not always monotonic as seen from the data.
- Increase in fuel thickness (h_{fu}) increases the burn rate and hence M_{pc}.
- Increase in pan diameter increases the burn rate and must be so reflected in M_{pc}.
- Decrease in pan wall thickness should result in reduced conductive flux and should be reflected in reduced M_{pc}.

Table 2. Properties of pan ($t_{cond} \sim h_{pan}^2/8\alpha_w$).

Material	d_{pan} mm	t_w mm	ρ_w kg/m^3	c_{pw} kJ/kg K	k_w W/m K	α_w mm^2/s	h_{pan} mm	t_{cond} s
AL	200	3	2730	0.91	60	24.1	40	8.5
MS	200	3	7800	0.46	32	8.9	40–60	22–100
SS	200	3	7800	0.46	16	4.45	40–60	44–200
SS [19]	200	3	7830	0.48	21	5.6	40	35
GL	190	3	2230	0.75	1.14	0.68	40	590

Table 3. Properties of the fuel.

Fuel	ρ_{fu} kg/m^3	T_{bfu} K	c_{pfu} kJ/kgK	L_{fu} kJ/kg	k_{fu} W/m.K	α_{fu} mm^2/s	μ_{fu} mNs/m^2	T_f K
n-heptane	680	369	2.1	322	0.14	0.090	0.409	1200

- Increase in initial fuel temperature increases the burn rate and hence M_{pc}.
- Increase in water depth over which fuel floats causes a reduction in burn rate and the effect asymptotes beyond some depth.

Rendering conductive heat transfer coefficient, k_w/h_{pan}, dimensionless is performed using the convective heat transfer coefficient, $h_{g,conv}$, which is obtained by expecting that the burn rate flux is controlled by convection in the early stages in a small diameter pan, in this case, 0.2 m dia, where radiational flux is minimal. This gives a value of 0.0045 kW/m^2 K. Subsequent burn rate simulations using an unsteady code [18] have confirmed this result. With regard to other dimensions – fuel thickness, free board, pan diameter and pan wall thickness, several possible dimensionless constructions are possible. The candidate for rendering the pan diameter dimensionless should arise from free convective length scale, $[v_g^2/g]^{(1/3)}$, where $v_g = \mu_g/\rho_g$ is the dynamic viscosity of the hot gases. With μ_g = 1.8 $\times 10^{-5}$ kg/m s, g = acceleration due to gravity = 9.8 m/s^2, this length scale is 0.21 m.

Much effort went into trying to find combinations of these quantities so that a parameter that can characterize the burn rate flux can be found. One of these that appeared to have minimum scatter of the data is a product of convective heat feed back to the fuel surface, which is constant for a range of pan diameters [18], and M_{pc} has been obtained. These parameters include most of the relevant fundamental parameters indicated in section 2 and two parameters, namely ρ_w and $c_{p,w}$, have been treated as fixed constants since it is taken that the pans are made of either SS or MS, for which the product $\rho_w c_{p,w}$ is the same. There are three dimensionless parameters P_1, P_2 and P_3 defined as follows.

The parameter P_1 is defined by

$$P_1 = \left[\frac{k_w}{h_{pan}h_{g,conv}}\frac{h_{fu}}{h_{fb}}\right]^{1/4}. \tag{1}$$

The parameter P_1 is chosen to account for conductive flux in addition to fuel depth effects. The first term in the bracket is discussed in the earlier paragraph. The role of h_{fb} vis-a-vis h_{fu} was deduced after trying out some options. The exponent was varied and the present choice of (1/4) provided a minimal deviation from the observed experimental dependence.

Parameter P_2 is defined by

$$P_2 = \left[1 - \exp(-0.25(d_{pan}/0.21)^{1.5}/P_1)(1 + 0.1(h_{wr}/h_{pan})^{2.3})\right]. \tag{2}$$

In this expression, the influence of the pan diameter is such that as it increases, one obtains an asymptotic value controlled by radiation through the exponential term. The exponent 1.5 on the pan diameter scaled by the convective length scale is chosen to provide the variation with diameter observed in the experimental data. It turns out that Ditch *et al* [16] have an exponent on pan diameter that is the same as here. This expression also accounts for water depth, h_{wr}, and it is scaled with pan depth.

Parameter P_3 is defined by

$$P_3 = \left[\frac{(T_{bfu} - T_0)}{(T_{bfu} - 300)}\frac{300}{T_{bfu}}\right]^{(-0.35)}. \tag{3}$$

This parameter accounts for the initial fuel temperature. It increases as the fuel temperature approaches the boiling point. They are now combined to obtain a parameter M_{pc} as

$$M_{pc} = P_1 P_3[1.5 + 8.5P_2]. \tag{4}$$

The data of mean burn flux of all the experiments with the data drawn from Chen *et al* [5, 6] are set out in figure 15. The mean mass burn flux can be set out as

$$\bar{m}''_{fu}(g/m^2 s) = [(h_{g,conv}(T_f - T_{bfu})/4L)M_{pc}. \tag{5}$$

As can be noted, the data-fit using the scaling laws appears to capture the behavior very well. A question will arise as to whether this is a simple curve fit or whether it qualifies to be a correlation. It would be a simple curve fit if its application was restricted to the present experimental data only. However it is to be noted that the fit uses fundamental parameters – properties of the fuel and material of the pan covering a wide range, and allows for asymptotic realization for large pan diameters as well. Also, not shown here, it works very well for other fuels like diesel, kerosene and alcohols. Since it covers all unsteady pool fires with commonly used pan materials and liquid fuels, it can be treated as a correlation.

Table 4 shows the results of effect of water on mean burn rate; the comparison between experiments and predicted values using correlation shows close agreement for most of the cases and for a few cases the error is large. It is evident that the proposed correlation is capable of providing reasonable estimates of the effect of water on burn flux as well.

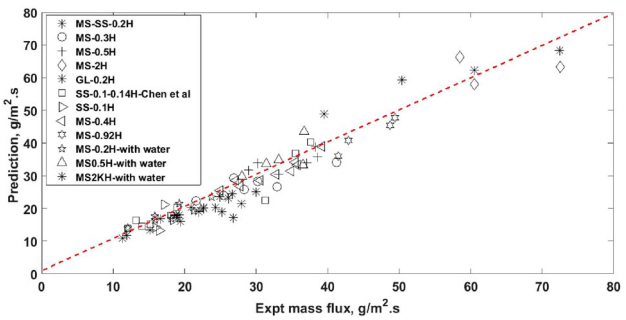

Figure 15. Experimental mass flux vs predicted mass flux; MS-0.3H implies 0.3 m dia mild steel pan with n-heptane fuel.

Table 4. $\bar{m}''_{fu}$ (g/m^{2}s) for 0.2 and 0.5 m dia MS pans; negble = negligible, implying the error is less than ± 5 %.

d_{pan} m	h_{pan} m	h_{fu} m	h_{wr} m	h_{fb} K	Expt g/m^{2}s	*Pred* g/m^{2}s	% Error –
0.2	0.06	0.01	0.01	0.04	18.1	16.8	+7
	0.06	0.01	0.02	0.03	15.9	17.6	−10.5
	0.06	0.02	0.01	0.03	22.4	20.9	−6.22
	0.06	0.02	0.02	0.02	19.3	21.4	−10.6
0.5	0.06	0.01	0.02	0.03	28	29.8	negble
	0.06	0.015	0.015	0.03	32	33.6	−6
	0.06	0.02	0.01	0.03	33.2	34.7	negble
	0.06	0.02	0.02	0.02	36.5	33.4	+9.6

6.1 *Pans of dia < 0.2 m*

Hayasaka [4] and Chen *et al* [5, 6] have experimented upon SS pans of 0.05, 0.1 and 0.141 m dia. Experiments were conducted here for comparison purposes with SS (present) and GL for 0.1 m dia. The predictions made using correlations are set out in Table 5. As can be noted, the predictions even for high fuel temperatures seem reasonable. Here again the predictions seem not unreasonable if we note that the methodology followed is the same as for larger diameter pans, the larger errors in the case of SS pans being related to this feature.

Table 5. $\bar{m}''_{fu}$ (g/m^{2}s) for 0.05, 0.1, 0.141 m dia SS (SS (present)) and GL – glass pans; negble = negligible, implying the error is less than ± 5 %.

d_{pan} m	h_{pan} m	h_{fu} m	h_{fb} m	T_0 K	Expt g/m^{2}s	*Pred* g/m^{2}s	% Error –
0.141	0.04	0.013	0.027	278	14.0	14.5	negble
Ref.[6]	0.04	0.013	0.027	290	15.2	15.2	negble
	0.04	0.013	0.027	319	18.1	17.8	negble
	0.04	0.013	0.027	343	31.2	28.1	+9.6
	0.04	0.013	0.027	365	40.2	40.2	negble
0.10	0.04	0.013	0.027	290	12.4	13.9	−13
Ref. [6]	0.04	0.013	0.027	319	13.4	16.3	−19
	0.04	0.013	0.027	343	19	20.3	negble
	0.04	0.013	0.027	365	36.8	35.5	negble
0.1	0.04	0.010	0.030	300	15.8	13.2	−28.7
Present	0.04	0.013	0.027	300	15.8	14.1	+12.8
SS	0.04	0.020	0.020	300	18.4	16.5	+11.2
	0.04	0.030	0.010	300	17.0	21	−18.5
0.1	0.04	0.010	0.030	300	10.1	8.2	−19.2
Present	0.04	0.020	0.020	300	10.8	9.0	−16.6
GL	0.04	0.030	0.010	300	11.9	9.6	−19.1
0.05 [4]	0.11	0.110	0.000	298	16.9	7.9	−28

7. Concluding remarks

The present study was initiated after noting that earlier literature has considerable data but many unresolved issues or conflicts. In order to determine the extent of influences of various controlling geometric and thermodynamic parameters, experiments were conducted over specifically designed pans with different depths and diameters from 0.1 to 2 m. The experiments have captured the data on mass burn vs time, wall tip temperatures, in-depth liquid temperatures to provide data for understanding and validation. They show that for small diameter pans of 0.2 m class, (a) the lowest fuel mass flux is 11 ± 2 g/m^{2}s for most pan materials, (b) the minimum flux is achieved for GL pan at 10 mm fuel depth and 2 mm depth in SS pan, (c) the minimum flux increases for MS and AL towards larger values, (d) fuel mass flux is less sensitive to fuel depths in GL pan, (e) fuel mass flux increases with SS and other metals to as high as 65 g/m^{2}s beyond about 20 mm fuel depth and this is related to wall conductivity heat inputs into the fuel that lead to bulk boiling and the highest possible burn rates and (f) free board effects are more significant at small pan diameters. To account for the effects of wall conductivity, fuel depth, free board and fuel temperature effects apart from the well-known pan diameter effect, a non-dimensional number M_{pc} has been evolved. The mean burn flux, $\bar{m}''_{fu}$, is correlated with this dimensionless number. This correlation gives a good estimate of the burn rate flux over the range of parameters. It is useful to point out that the correlation has been tested and found to work well for other fuels also even though this paper has presented the data on n-heptane only.

Acknowledgements

The authors are thankful to the authorities of Jain Deemed to be University for encouragement in the conduct of this research.

List of symbols

A_1	Cross sectional area (m)
AL	Aluminum alloy
C_{pw}	Specific heat (kJ/kgK)
d_{pan}	Diameter of pan (m)
dia	Diameter of pan (m)
GL	Glass
h_{pan}	Height of pan (m)
h_{fu}	Depth of fuel (m)
h_{wr}	Depth of water below the fuel (m)
h_{fb}	Height of free board (m)

$h_{g,conv}$	Convective heat transfer coefficient in gas phase (kW/m^2 K)
L_{fu}	Latent heat of vaporization of the fuel (kJ/kg)
k_w	Thermal conductivity of pan (kW/m.K)
$\bar{m}''_{fu}$	Mean mass flux (kg/m^2s)
M_{pc}	Dimensionless pan burn number
MS	Mild steel
SS	Stainless steel
T_p	Pan tip temperature (K)
T_{wb}	Bottom outer wall temperature (K)
T_f	Flame temperature (K)
T_{bot}	Fuel bottom temperature (K)
T_s	Fuel surface temperature (K)
ρ_{fu}	Density of fuel (kg/m^3)
α_{fu}	Thermal diffusivity of fuel (m^2/s)

References

[1] Hottel H C 1958 Certain laws governing diffusive burning of liquids – a review. *Fire Res. Abstr. Rev.* 1: 41–44

[2] Blinov V I and Khudiakov G N 1961 *Diffusion burning of liquids*. Report No. AD296762, Moscow Academy of Sciences, U S Army Engineering Research and Development Laboratories, Fort Belvoir, Virginia

[3] Babrauskas V 1983 Estimating large pool fire burning rates. *Fire Technol.* 19: 251–261

[4] Hayasaka H 1997 Unsteady burning rates of small pool fires. *Fire Saf. Sci.* 5: 499–510

[5] Chen B, Shouxiang Lu, Changhai Li, Quansheng K, and Man Yuan 2012 Unsteady burning of thin-layer pool fires. *J. Fire Sci.* 30: 3–15

[6] Chen B, Shou-Xiang Lu, Chang-Hai Li, Quan-Sheng K, and Vivien Lecoustre 2011 Initial fuel temperature effects on burning rate of pool fire. *J. Hazard. Mater.* 188: 369–374

[7] Nakakuki A 1994 Heat transfer mechanisms in liquid pool fires. *Fire Saf. J.* 23: 339–363

[8] Nakakuki A 2002 Heat transfer in pool fires at a certain small lip height. *Combust. Flame* 131: 259–272

[9] Dlugugorski B Z and Wilson M 1995 Effect of lip height on properties of small scale pool fires. *Fire Saf. Sci.* 2: 129–140

[10] Hamins A, Fischer S J, Kashiwagi T, Klassen M E, and Gore J P 1994 Heat feedback to the fuel surface in pool fires. *Combust. Sci. Technol.* 97: 37–62

[11] Klassen M E and Gore J P 1994 *Structure and radiation properties of pool fires*. Report No. NIST-GCR-94-651, National Institute of Standards and Technology, Gaithersburg, MD

[12] Gregory J J, Keltner N R, and Mata R 1989 Thermal measurements in large pool fires. *J. Heat Transfer* 111: 446–454

[13] Koseki H 1989 Combustion properties of large liquid pool fires. *Fire Technol.* 25: 241–255

[14] Hayasaka H 1994 A study on pool flame structure using thermography. *Fire Saf. Sci.* 4: 125–136

[15] Blanchat T K and Anttila J S 2011 *Hydrocarbon characterization experiments in fully turbulent fires – results and data analysis*. Report No. SAND2010-6377, Sandia National Laboratories, Albuquerque, NM

[16] Ditch B D, de Ris J L, Thomas K B, Marcos C, Robert G B, and Sergey B D 2013 Pool fires – an empirical correlation. *Combust. Flame* 160: 2964–2974

[17] Weckman E J and Strong A B 1996 Experimental investigation of the turbulence structure of medium scale methanol pool fires. *Combust. Flame* 105: 245–266

[18] Mukunda H S, Shivakumar A, Sowriraajan A Ve, and Dixit B S 2019 *Unsteady pool fires – fuel depth and pan wall effects – experiments and modeling*. FCRC Report 1902, Fire and Combustion Research Centre, Jain (deemed-to-be-university), Bangalore